J Mater Sci: Mater Med (2008) 19:2983–2992
DOI 10.1007/s10856-007-3045-2

Bone ingrowth in zirconia and hydroxyapatite scaffolds with identical macroporosity

Johan Malmström · Erik Adolfsson · Lena Emanuelsson · Peter Thomsen

Received: 29 March 2006 / Accepted: 5 May 2006 / Published online: 5 May 2007

Abstract The role of the material composition, porosity and surface topography of scaffolds for promotion of osteogenesis and osseointegration is not fully understood. The aim of the present study was to evaluate the effects of material composition and surface topography on bone ingrowth and bone contact. Designed macroporous ceramic scaffolds of zirconia and hydroxyapatite were used. Using free form fabrication (FFF) techniques an identical macroporosity in both materials was achieved. The scaffolds were implanted in rabbit tibia (cortical bone) and femur (trabecular bone). After 6 weeks of implantation the tissue response was assessed with histology and histomorphometry. The results showed significantly more bone ingrowth and bone contact in the hydroxyapatite scaffolds compared to the zirconia scaffold. Surface topography had no significant effect on bone contact inside the macropores regardless of material. This was observed in both cortical and trabecular bone sites. The study suggests that the difference between hydroxyapatite and zirconia was due to a difference in material chemistry.

Introduction

Bone defects occur in a variety of clinical situations, and their reconstruction to provide mechanical integrity to the skeleton is a necessary step in the patient's rehabilitation. A problem or disadvantage frequently dwelt upon in the clinical literature describing the use of hydroxyapatite granules is the difficulty of holding the material in place during and immediately after surgery. To overcome such problems, other types of material have been added to fixate the granules during an initial healing stage, before and while bone growth is induced, to form a framework of ''trabecular'' bone holding the pieces together. Calcium sulphate [1–3], bioglass particles [4, 5], and calcium phosphates [6], alone or in combinations [7, 8], have all been used for this purpose. A way to minimize the risk of disintegration of the implanted bone substitute after surgery is to produce a continuous porous material that holds together, acting as a unit.

To produce continuous porous scaffolds for bone regeneration, several conventional ceramic processing techniques have been used such as foaming of ceramic suspensions [9], adding fugitive materials to the ceramic powder or infiltrating reticulated polymer foams with a ceramic suspension [10].

There are also techniques that exploit naturally occurring porous calcium-based structures, as in the hydrothermal conversion of either coral [11] or bone [12]. However, the traditional ceramic processing methods, the naturally occurring calcium-based structures and the organic particle embedding technique, provide very limited control over the internal architecture of the material [13–16]. Apart from a biocompatible scaffold material the scaffolds are further required to have a suitable design that will promote the complete infiltration of bone tissue, bone marrow and blood vessels as occurs when autograft and allografts are used. Optimal pore size for tissue ingrowth is rarely defined and the intervals mentioned are quite variable causing confusion about the mechanisms behind osseointegration

J. Malmström (✉) · LenaEmanuelsson · P. Thomsen
Department of Biomaterials, Institute of Surgical Sciences, Sahlgrenska Academy, Box 412, 405 30 Gothenburg, Sweden
e-mail: Johan.Malmstrom@biomaterials.gu.se

E. Adolfsson
Swedish Ceramic Institute, Goteborg, Sweden

within macroporous structures. A pore size >100–150 μm is often cited as a minimum to facilitate ingrowth of mineralized bone [17–20]. However, other researchers have promoted the importance of additional structural parameters, such as pore morphology, percent porosity, pore connectivity and surface topography [15, 21–26] to affect bone ingrowth and implant integration.

To avoid a randomly shaped pore structure, other fabrication techniques need to be introduced. One such technique is free form fabrication where a model that represents the desired shape of the scaffold is drawn with a CAD tool. From a model the real scaffold is fabricated where both the external and the internal shapes can be controlled. The introduction of these fabrication methods to produce defined scaffolds makes it further possible to fabricate designed materials that can be used as research tools to evaluate not only the influence of porosity but also the effect of different material compositions. Previously performed experimental studies evaluating the bone response to different ceramic materials have presented results which may not only depend on the material composition but also on the experimental design or influence from other properties of the used ceramics [27–29].

In the present study ceramic scaffolds were fabricated as a continuous structure prior to implantation. The aim was to produce scaffolds of zirconia and hydroxyapatite with an identical interconnected macroporosity and to evaluate how the material influenced the initial bone ingrowth and contact in an experimental animal model.

Materials and methods

Material

A CAD tool (Solid Works, USA) was used to design models of scaffolds with squarely shaped and interconnected pore channels (Fig. 1). Moulds corresponding to the designed macroporosities were built with free form fabrication equipment (Model Maker II, Sanders, USA) using an inkjet printing principle with a layer thickness of approximately 50 μm. A thermoplastic building material (Proto build, Sanders, USA) was used for the mould structure, surrounded by a supporting wax-based material (Proto support, Sanders, USA), allowing overhangs to be built. The support material was separately removed from the mould, leaving a structure of build material corresponding to the macroporosity of the scaffold designed with the CAD tool. The free form fabricated moulds were infiltrated with ceramic suspensions prepared by ball milling of hydroxyapatite (HA) (Plasma Biotal, UK) and zirconia (ZrO_2) (Tosoh, Japan) with a solids loading of 45 vol% and 50 vol%, respectively. In order to improve the green strength of the brittle cast materials a binder (LDM7651S, Clariant, Sweden) was added to the suspensions. The ceramic suspensions were consolidated using slip casting (colloidal filtration) where the excess of water was drained from the suspension on a plate of plaster. The cast materials were heated with a low heating rate of 1 °C/min up to 600 °C to burn away the mould and organic additives, and 5 °C/min up to the sintering temperature, 1,300 °C for hydroxyapatite and 1,500 °C for zirconia that was kept for 2 h before the temperature was decreased by 5 °C/min. The bulk density of dense sintered material was measured by Archimedes' principle and the macroporosity of the scaffold was calculated from the geometrical dimensions of the macroporous structures. The phase present in zirconia and apatite were characterized by their x-ray diffraction (XRD) patterns obtained in a Guinier-Hägg camera, using CuKα_1 radiation.

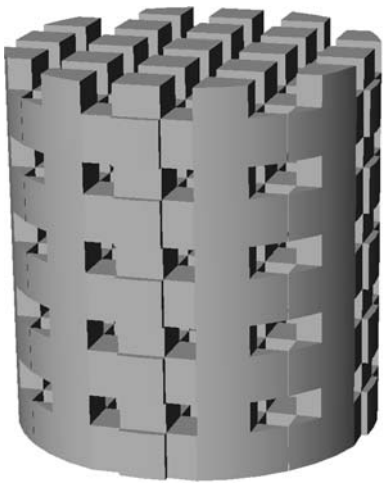

Fig. 1 CAD-illustration of the scaffold

Surface topography

The topography of the sintered materials was studied by scanning electron microscopy (SEM) and optical interferometry (MicroXAM^{TM}, PhaseShift, Tucson, USA). The interferometry analysis was performed with a 50× objective and a zoom factor of 0.625, resulting in a measurement area of 200 × 260 μm^2. In total three specimens of each type of material were used for the topographical characterisation. Interferometer measurements were made on beam surfaces of each material representing two sides. Here on referred to as (A) and (B) sides of the macropore (Fig. 2). The topography of (A) and (B) sides was described as the mean of 30 measurements for each surface and material resulting in two surface roughness values for each scaffold material. The errors of form were removed with a digital Gaussian filter sized 50 × 50 μm^2 before calculating the following topographical parameters: (1)

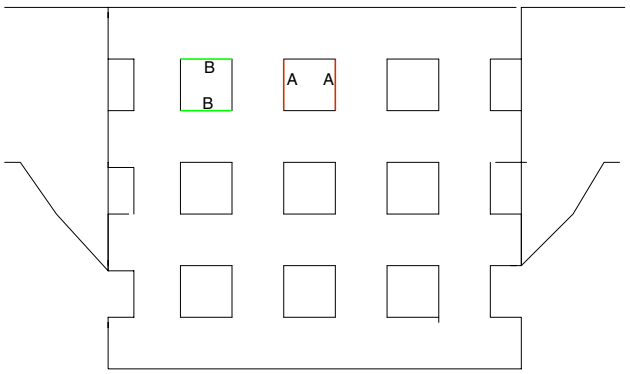

Fig. 2 Schematic picture demonstrating A and B sides inside macropore. Representing different surface roughness values

S_a—the average height of structures from a mean plane; (2) S_{ds}—the number of peaks per unit area; (3) S_{dr}—the developed surface ratio; (4) S_{tr}—texture aspect ratio used to separate isotropy and anisotropy of surfaces; (5) S_{ci}—the core fluid retention index.

Surgery

According to a randomised implant insertion scheme, 32 scaffolds (16 of each type) were placed in eight female adult New Zealand white rabbits, weighing 4.4–5.6 kg and fed ad libitum. Scaffold diameter was 3.8 mm and height 4 mm. The experiments were approved by the Local Ethics Committee, Göteborg University (237-2001). Prior to surgery, the animals were anaesthetized by intramuscular (i.m.) injections of a combination of phentanyl and fluanizon (Hypnorm®, Janssen, Brussels, Belgium; 0.7 mg/kg body weight (b.wt.) and intraperitoneal (i.p.) injection of diazepam (Stesolid®, Dumex, Copenhagen, Denmark; 1.5 mg/kg b.wt.) Lidocaine (5% Xylocain®, Astra AB Södertälje, Sweden) was infiltrated subcutaneously (s.c.) to obtain local anaesthesia. The limbs were shaved and disinfected with chlorohexidine (5 mg/ml, Pharmacia AB, Stockholm, Sweden). Operations were performed under sterile conditions. Each animal received two scaffolds of the same type in one leg and two scaffolds of the other type in the contra lateral leg. One scaffold was inserted in each proximal tibial metaphysis and one scaffold in each medial femoral condyle according to a random scheme. The bone was exposed separately through skin incisions and blunt dissection of the underlying tissue, including the periosteum. The holes in both the tibia and femur were made using dental implantation drills up to a diameter of 3.8 mm under profuse irrigation with sterile saline (NaCl 9 mg/ml; ACO, Sweden). The scaffolds were then gently pressed in place. The operation site was rinsed with saline and the tissues were sutured in separate layers with Vicryl® 5-0 and finally intracutaneous with Monovicryl® 4-0. Animals were given trimetoprim 40 mg + sulfadoxin 200 mg/ml (Borgal® vet, Hoechst AB) prior to surgery and 2 days postoperatively. Analgetics, buprenorphine (Temgesic®, Reckitt and Colman, USA, 0.05 mg/ml), were given during 3 days postoperatively.

Animal sacrifice

Animals were killed after 6 weeks with an overdose of barbiturate (Mebumal®, ACO Läkemedel AB, Solna, Sweden) and fixed by perfusion via the left heart ventricle with 2.5% glutaraldehyde in 0.05 M sodium cacodylate buffer, pH 7.4. The scaffolds and the surrounding bone were removed en bloc, and further immersed in glutaraldehyde for 2–4 days. After dehydration in ethanol, the undecalcified specimens were embedded in plastic resin (LR White, the London Resin Co Ltd, Hampshire, UK). The specimens were divided longitudinally by sawing—in centre of scaffold (Exact cutting and grinding equipment, Exact Apparatebau, Norderstedt, Germany) and ground sections (thickness:15–20 μm) prepared and stained with 1% toluidine blue [30, 31].

Microscopy and morphometry

Light microscopic morphometry was performed on the ground sections using a Nikon Eclipse E600 light microscope and connected computer software. Evaluation was performed by measuring the bone ingrowth and bone-to-scaffold contact inside all scaffolds. Also evaluation of bone-to-scaffold contact between (A) and (B) sides of the macropores for respective material was performed.

Statistics

The Wilcoxon signed rank sum test was used for statistical analysis. $p < 0.05$ (*) and $p < 0.001$ (**) were set for significant differences.

Results

Material

The cast materials of hydroxyapatite had a green density of 65% and zirconia of 55% and when sintered both materials reached densities above 98%. The total shrinkage of the cast materials during the sintering process was then slightly different. To compensate for the different shrinkages, the size of the free form fabricated moulds was rescaled individually for each material. This made it possible to fabricate macroporous scaffolds of two different materials with an identical macroporosity, consisting of squarely shaped

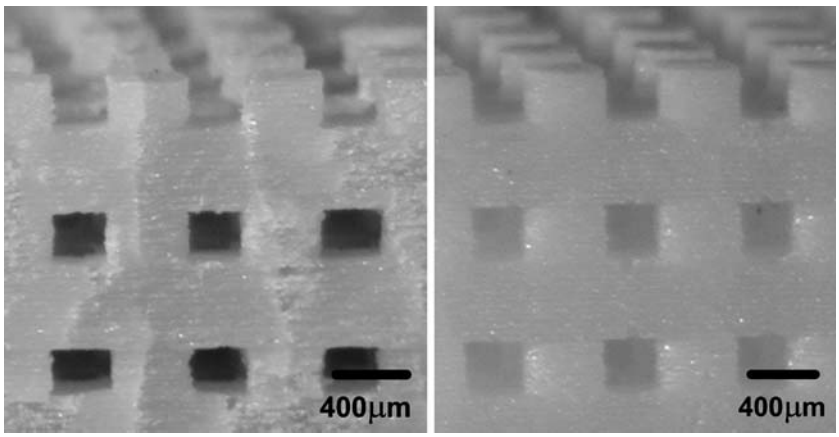

Fig. 3 (**A**, **B**) Macroporosity of hydroxyapatite and zirconia scaffolds. Bar = 400 µm

and interconnected pore channels with a size around 350 µm and a macroporosity around 40 vol% (Fig. 3). The minor remaining porosity was due to closed pores without any connection to the external surface. The XRD analysis of the hydroxyapatite showed the presence of minor amount of β-TCP, whereas the zirconia was mainly tetragonal. A small amounts of the tetragonal phase was transformed to monoclinic when the dense material was crushed to powder during sample preparation (Fig. 4).

Surface topography

The (A) sides were rougher than the (B) sides inside the macropores irrespective of material, with respect to the S_a value. No differences in roughness could be seen comparing the (A)-sides between the two materials. The same was seen for the (B)-sides. In hydroxyapatite a surface enlargement for the (A)-sides was noted compared to zirconia (A)-sides, as characterised by S_{dr}. A clear orientation of structures could be distinguished for both sides and both materials (S_{tr}) (Table 1). The surfaces of the two materials are visualized in (Fig. 5A–D).

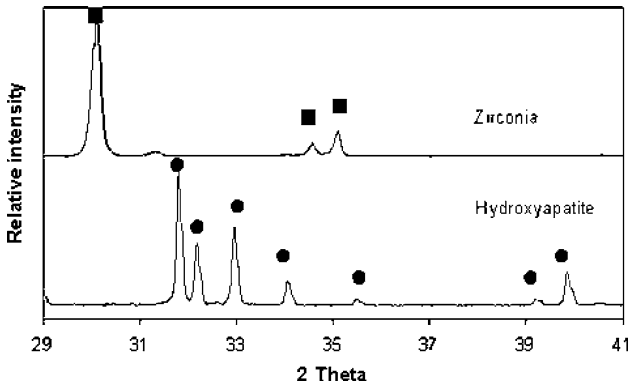

Fig. 4 X-ray diffraction patterns of zironia and hydroxyapatite: (■) tetragonal zirconia and (•) hydroxyapatite

Morphology

All sites healed uneventfully, showing no clinical evidence of inflammatory response to the ceramic scaffold during the experimental period. All scaffolds were well incorporated after 6 weeks. In some instances bone covered the scaffolds. In general the interface between host/scaffold and the defect border was evident. In tibia the newly formed bone appeared to have its origin from the endosteal part of the bone and from the defect border. The areas inside the scaffolds were filled with irregular, woven bone. Blood vessels were detected in the newly formed bone inside the macropores. Irregular, woven bone was also seen as bone trabeculae reaching the scaffolds from the adjacent bone. Bone was often in contact with the surface of the scaffold both inside the macropores and externally. Bone followed the irregularities of the surface of the scaffold irrespective of material and surface roughness (Figs. 6C, F, 7C, F). Bone resorption and remodelling was evident in the adjacent

Table 1 Surface roughness for zirconia (ZrO_2) and hydroxyapatite (HA) representing (A) and (B) sides inside macropores

	Side	S_a (µm)	S_{ds} (μm^{-2})	S_{dr} (%)	S_{tr}	S_{ci}
ZrO_2	A	2.23 (0.78)	0.094 (0.014)	33.85 (13.57)	0.10 (0.03)	1.53 (0.09)
	B	0.51 (0.16)	0.149 (0.011)	9.91 (2.59)	0.17 (0.21)	1.40 (0.15)
HA	A	2.54 (0.63)	0.105 (0.008)	200.66 (69.88)	0.46 (0.16)	1.40 (0.20)
	B	0.44 (0.10)	0.128 (0.016)	16.72 (5.35)	0.24 (0.18)	1.24 (0.11)

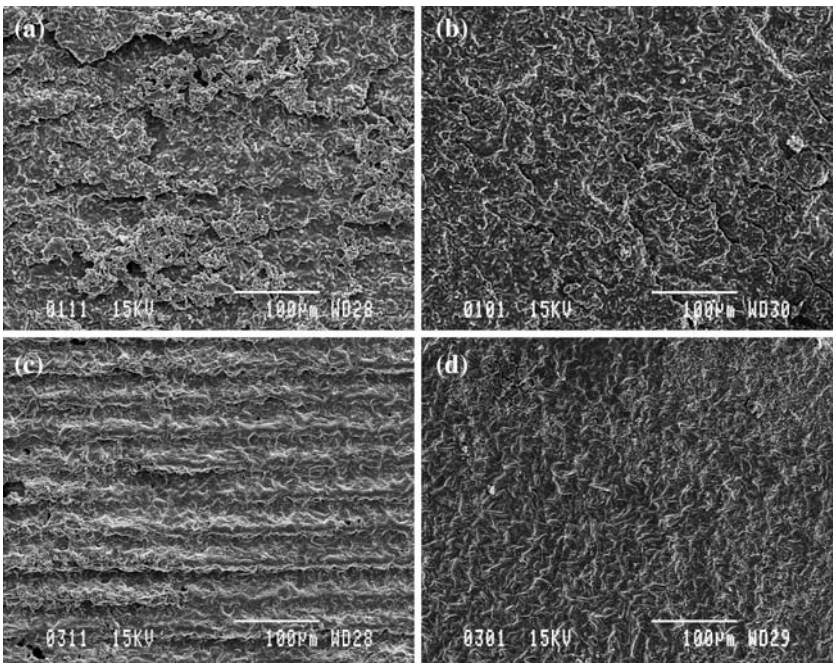

Fig. 5 (**A**) Topography of side (A) hydroxyapatite. Bar = 100 µm. (**B**) Topography of side (B) hydroxyapatite. Bar = 100 µm. (**C**) Topography of side (A) zirconia. Bar = 100 µm. (**D**) Topography of side (B) zirconia. Bar = 100 µm

mature bone (Fig. 6A, D). Endosteal bone growth was more evident externally and interiorly of scaffolds located in the femur than in the tibia. This was notable in particular for hydroxyapatite scaffolds. Two different general morphological patterns of bone were observed. In the hydroxyapatite scaffolds the internal macroporosities had bone lining the inner surface of the scaffolds as well as filling the centre portions of the porosities. In contrast, bone was usually observed only as a lining of the inner surface of the internal macroporosities of zirconia. In areas devoid of mineralized bone, bone marrow and/or adipose tissue were detected.

Morphometry

After 6 weeks the amount of bone area and bone-to-scaffold contact within scaffolds was significantly higher for the hydroxyapatite-group compared to the zirconia-group (Fig. 8, 9, 10, 11). The tibia scaffolds had a mean bone area within the scaffolds of 36% for hydroxyapatite and 13% for zirconia. In femur the mean bone area within the hydroxyapatite scaffold was 39% and for zirconia 13%. The mean bone-to-scaffold contact after 6 weeks in the tibia was 41% for hydroxyapatite and 12% for zirconia. In femur the mean bone-to-scaffold contact for hydroxyapatite was 49% and for zirconia 24%. The two different surface topographies were not found to affect the bone contact in either zirconia or hydroxyapatite bone scaffolds (Figs. 12A, B, 13A, B).

Discussion

In the present study, scaffolds of two different materials, hydroxyapatite and zirconia, with an identical interconnected macroporosity were evaluated during the initial phase of healing in bone. The mechanism whereby ceramics stimulate new bone formation is not altogether known. Although it is recognised that both the rate and the final volume of regenerated bone may be primarily dependent on various features of the macroporosity, such as volume fraction, pore size and pore connectivity, the exact effect of chemistry has been hard to evaluate due to difficulties in manufacturing identical scaffolds [13, 32–36]. To evaluate the effect of different scaffold material chemistries it is required that the scaffolds have the same geometrical characteristics in order to exclude confounding factors. In the present study this was possible using a free form fabrication technique to produce identical macroporous scaffolds with the same external shape, inner macroporous shape, size and interconnectivity. The developed fabrication process made it further possible to reach almost fully dense materials. The small amount of remaining microporosity, consisted of closed pores and would thus not influence the biological response. The control of the scaffolds permitted the evaluation of the effect of different material chemistries on the amount and pattern of bone ingrowth into scaffolds in vivo.

In the present study, the implantation of hydroxyapatite scaffolds resulted in a significantly higher quantity of bone at 6 weeks compared to zirconia. Furthermore, a

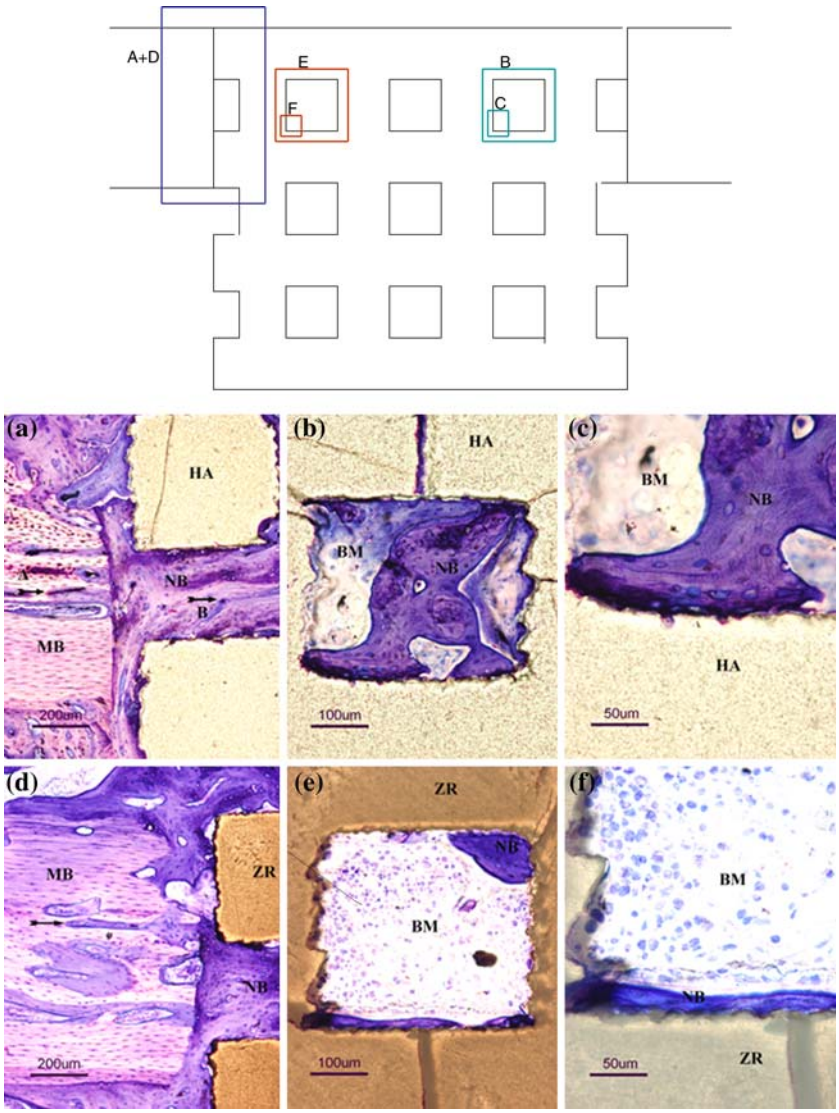

Fig. 6 Mount of light micrographs (ground sections) of scaffolds in tibia located according to schematic picture (insert, top): (**A**) Hydroxyapatite (HA), 6 weeks. Defect border where arrow A denotes bone remodelling in mature bone (MB). Arrow B denotes blood vessel in newly formed bone (NB). Bone has established contact with the outer surface of the scaffold and the inner surface of the macropore. Bar = 200 µm. (**B**) Hydroxyapatite, 6 weeks. Macropore inside scaffold which is being filled with newly formed bone (NB) and bone marrow (BM). Bar = 100 µm. (**C**) Hydroxyapatite, 6 weeks. Newly formed bone (NB) is closely lining the irregularities inside the macropore. Bar = 50 µm. (**D**) Zirconia (ZR), 6 weeks. Defect border where arrow denotes bone remodelling in mature bone (MB). Newly formed bone (NB) is observed inside a pore opening in the scaffold. Bone has established focal contacts with the outer surface of the Zirconia scaffold. Bar = 200 µm. (**E**) Zirconia, 6 weeks. Macropore inside implant lined by newly formed bone (NB) and mostly filled by bone marrow (BM). Bar = 100 µm. (**F**) Zirconia, 6 weeks. Newly formed bone (NB) is closely lining the surface irregularities inside the macropore. Bar = 50 µm

significantly higher degree of bone to scaffold contact was observed in hydroxyapatite scaffolds at 6 weeks in comparison to zirconia. The effect on bone contact by different surface topographies inside the macropores for each material were not significant. This has earlier been shown by Sennerby et al. comparing zirconia dental implants with different surface topographies [37]. Analysis of the pattern of bone ingrowth was possible because of the high controllability of the scaffolds. Marked differences in the distribution of newly formed bone inside the scaffolds were demonstrated between the two materials. The results suggest that the bone formation inside an implanted scaffold is more strongly influenced by the effect of the material chemistry of the scaffold than by the osteogenic capacity of the different bone beds. The results in this study might be explained by the presented theory that calcium phosphate (CaP) biomaterials have the ability to form bone apatitelike material or carbonate hydroxyapatite on their surfaces [38].

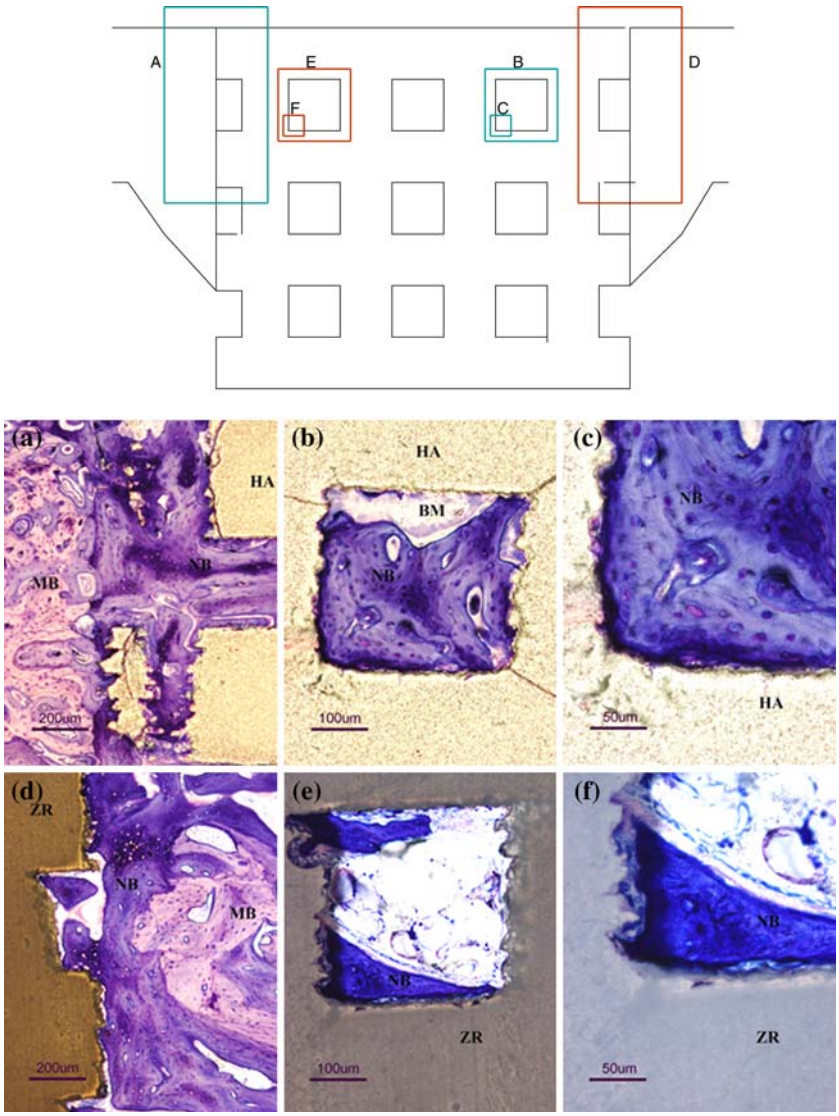

Fig. 7 Mount of light micrographs (ground sections) of scaffolds in femur located according to schematic picture (insert, top): (A) Hydroxyapatite (HA), 6 weeks. Defect border of mature bone (MB) undergoing remodelling. Newly formed bone (NB) in the defect border is reaching into the macropore and has established contact with the outer surface of the scaffold. Bar = 200 μm. (**B**) Hydroxyapatite, 6 weeks. Macropore inside scaffold is being filled with newly formed bone (NB) and bone marrow (BM). Bar = 100 μm. (**C**) Hydroxyapatite, 6 weeks. Newly formed bone (NB) is lining the macropore and almost entirely occupying the inner pore volume. Bar = 50 μm. (**D**) Zirconia (ZR), 6 weeks. Defect border consisting of mature (MB) and newly formed bone (NB). The area is undergoing an intense remodelling. The newly formed bone is reaching the surface of the zirconia scaffold and appears to be in a direct contact at several locations. Bar = 200 μm. (**E**) Zirconia, 6 weeks. The luminal surfaces of a macropore inside scaffold has a lining of newly formed bone (NB) whereas the main portion of the pore is filled with bone marrow. Bar = 100 μm. (**F**) Zirconia, 6 weeks. Detail showing the close contact between the newly formed bone and the surface of the macropore. Bar = 50 μm

In vivo, the formation of carbonateapatite on surfaces of CaP biomaterials at the bone-biomaterial interface is thought to be a cell-mediated dissolution and precipitation processes. Ca and P ions, liberated in the microenvironment by cellular activity, become incorporated in the carbonate hydroxyapatite. This initial action may trigger a mineralization of the extracellular matrix leading to bone formation. The enrichment of Ca and P ions in the microenvironment seems to promote bone mineralization and enhance bone formation [38]. Another possibility is that ceramic materials may induce different protein adsorption, which in turn could enhance cell adhesion and integration of bone cells [39]. On the other hand, suggestions have been made for hydroxyapatite and zirconia that despite their physico-chemical differences they both display low binding capacities and approximately the same

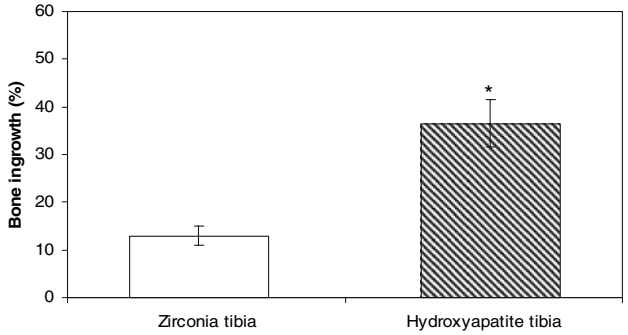

Fig. 8 Hydroxyapatite versus zirconia *$p < 0.05$

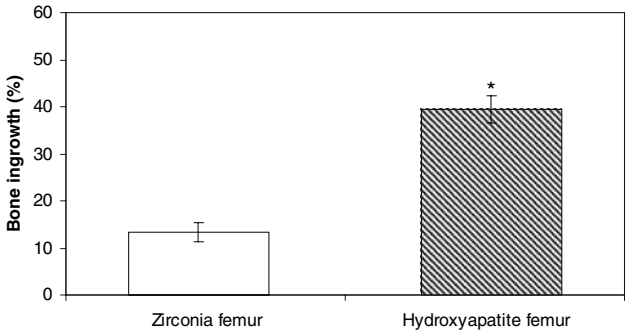

Fig. 9 Hydroxyapatite versus zirconia *$p < 0.05$

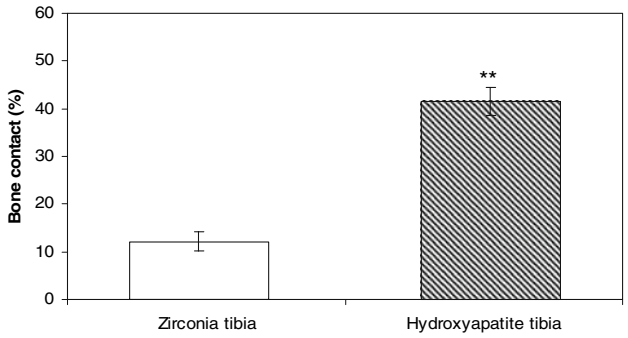

Fig. 10 Hydroxyapatite versus zirconia **$p < 0.001$

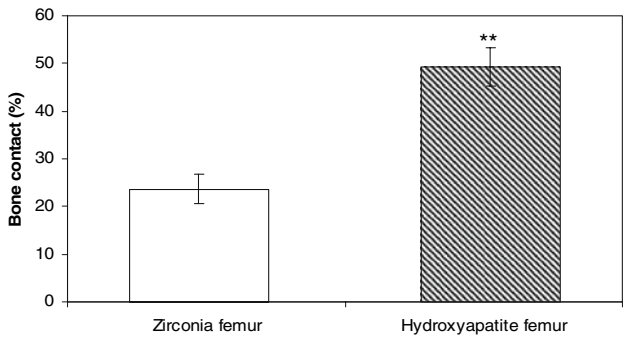

Fig. 11 Hydroxyapatite versus zirconia **$p < 0.001$

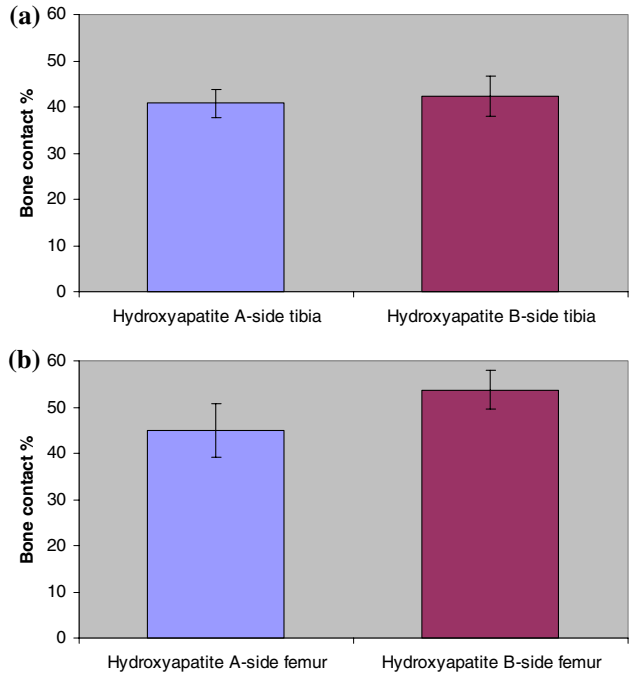

Fig. 12 (**A**) The relative proportion (%) of bone-to-scaffold contact of (A) and (B) pore surfaces within hydroxyapatite macroporous scaffolds in tibia at 6 weeks. No significant difference was demonstrated. (**B**) The relative proportion (%) of bone-to-scaffold contact of (A) and (B) pore surfaces within hydroxyapatite macroporous scaffolds in femur at 6 weeks. No significant difference was demonstrated

adsorption behaviour for plasma proteins [40]. Biomaterials may initiate several and complex biological reactions in the host tissue and the cell-biomaterial contact can evoke the release of chemotactic mediators and growth factors that may elicit and sustain inflammatory responses at the implant site [41].

Our results demonstrate that hydroxyapatite as a scaffold material promotes early bone ingrowth and bone contact as observed after 6 weeks compared to zirconia. Further, the chemistry of the scaffold material strongly influences the bone response in both cortical and trabecular bone. A prerequisite for this conclusion is that other scaffold properties of importance for bone ingrowth like pore connectivity, pore morphology (shape and size) and percent porosity were identical for hydroxyapatite and zirconia. The current free form fabrication technique can provide controlled geometry designs with specified chemical properties, and implicitly, this could open a door to study the effect of the internal scaffold architecture design with other essential properties, such as chemistry, kept in a controlled manner. Another advantage of designed scaffolds is the ability to customize scaffolds for anatomical defects.

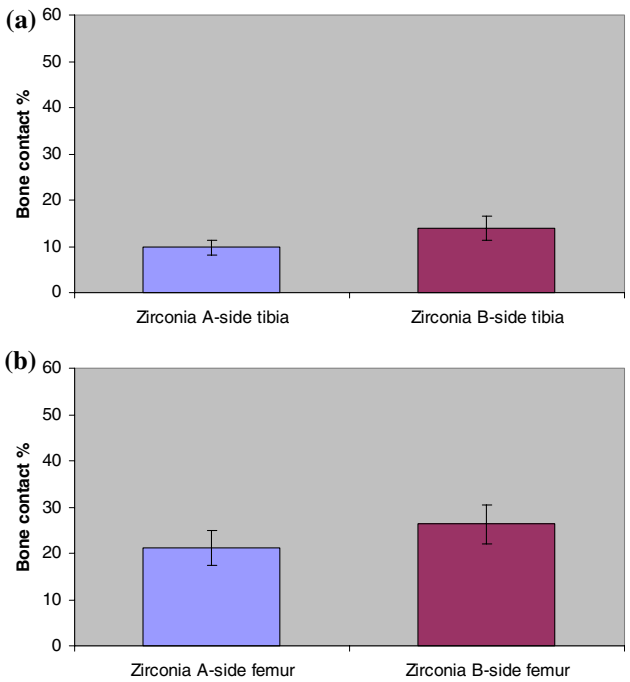

Fig. 13 (**A**) The relative proportion (%) of bone-to-scaffold contact of (A) and (B) pore surfaces within zirconia macroporous scaffolds in tibia at 6 weeks. No significant difference was demonstrated. (**B**) The relative proportion (%) of bone-to-scaffold contact of (A) and (B) pore surfaces within zirconia macroporous scaffolds in femur at 6 weeks. No significant difference was demonstrated

Conclusions

(1) Macroporous scaffolds with identical macroporosity have been produced in hydroxyapatite and zirconia using a free form fabrication technique. The fabrication technique of designed scaffolds holds promise as a valuable tool for evaluating tissue-material interactions.

(2) Evaluating the bone response within identical scaffolds of hydroxyapatite and zirconia, the significant differences in both cortical and trabecular bone in favour of hydroxyapatite is likely to be related to differences in the material chemistry of the two scaffolds. The bone contact in scaffolds of zirconia and hydroxyapatite was not found to be influenced by the two different surface topographies.

Acknowledgments This study was supported by the VINNOVA Vinn Växt Program, Biomedical Development in Western Sweden, Institute for Biomaterials and Cell Therapy (IBCT), the Swedish Research Council (grant K2006-73X-09495-16-3) and the Hjalmar Svensson Foundation. The authors thank Dr Anna Arvidsson, Dr Göran Wetter and Dr Magnus Hakeberg.

References

1. J. W. FRAME, *J. Dent.* **3** (1975) 177
2. R. GUARNIERI and M. BOVI, *Int. J. Periodontics Restorative Dent.* **22** (2002) 503
3. D. De LEONARDIS and G. E. PECORA, *Int. J. Oral Maxillofac. Implants* **14** (1999) 869
4. M. M. AMATO and S. M. BLAYDON, *Ophthal. Plast. Reconstr. Surg.* **19** (2003) 455
5. C. I. KNAPP and F. FEUILLE, *Int. J. Periodontics Restorative Dent.* **23** (2003) 129
6. E. LILJENSTEN and E. ADOLFSSON, *Clin. Implant Dent. Relat. Res.* **5** (2003) 95
7. H. OONISHI and S. KUSHITANI, *Clin. Orthop.* issue no. (334) (1997) 316
8. D. STUBBS and M. DEAKIN, *Biomaterials* **25** (2004) 5037
9. W. MINNEAR, in M. J. CIMA (ed), Ceramics Transactions 26, Forming Science and Technology for Ceramics (The American Ceramic Society, Westerville, 1992) p. 150
10. S. V. SCHWARTZWALDER, U.S. Pat. No. 3090094 (1963)
11. D. M. ROY and S. K. LINNEHAN, *Nature* **247** (1974) 220
12. B. A. DARD and M. LIEBENDORGER, *Act Odonto Stom* **185** (1994) 61
13. A. BIGNON and J. CHOUTEAU, *J. Mater. Sci. Mater. Med.* **14** (2003) 1089
14. Z. ARTZI and A. KOZLOVSKY, *J. Clin. Periodontol.* **32** (2005) 193
15. J.-H. KUHNE, R. B. BARTL and B. FRISCH, *Acta Orthop Scand* **65** (1994) 246
16. V. M. RUSU, C. H. NG and M. WILKE, *Biomaterials* **26** (2005) 5414
17. A. UCHIDA and S. NADE, *J. Orthop. Res.* **3** (1985) 65
18. K. SHIMAZAKI and V. MOONEY, *J. Orthop. Res.* **3** (1985) 301
19. R. E. HOLMES and R. W. BUCHOLZ, *J. Orthop. Res.* **5** (1987) 114
20. G. DACULSI and N. PASSUTI, *Biomaterials* **11** (1990) 86
21. J. J. KLAWITTER and S. F. HULBERT, *J. Biomed. Mater. Res.* **5** (1971) 161
22. P. S. EGGLI and W. MULLER, *Clin. Orthop.* issue no. (232) (1988) 127
23. J. X. LU and B. FLAUTRE, *J. Mater. Sci. Mater. Med.* **10** (1999) 111
24. K. A. HING and S. M. BEST, *J. Mater. Sci. Mater. Med.* **10** (1999) 663
25. K. A. HING and S. M. BEST, *J. Biomed. Mater. Res. A* **68** (2004) 187
26. A. WENNERBERG, Thesis, University of Göteborg, Sweden 1996., 1996
27. P. FRAYSSINET and J. L. TROUILLET, *Biomaterials* **14** (1993) 423
28. Y. S. CHANG and M. OKA, *J. Biomed. Mater. Res.* **30** (1996) 117
29. Y. IWASHITA and T. YAMAMURO, *J. Appl. Biomater.* **3** (1992) 259
30. K. DONATH and G. BREUNER, *J. Oral. Pathol.* **11** (1982) 318
31. K. DONATH, *Der Präparator* **34** (1988) 318
32. P. HABIBOVIC and H. YUAN, *Biomaterials* **26** (2005) 3565
33. K. A. HING and S. M. BEST, *J. Mater. Sci. Mater. Med.* **10** (1999) 135
34. J. L. SIMON and T. D. ROY, *J. Biomed. Mater. Res. A* **66** (2003) 275
35. S. LI and J. R. De WIJN, *Tissue Eng.* **9** (2003) 535
36. M. BOHNER and G. H. van LENTHE, *Biomaterials* **26** (2005) 6099

37. L. SENNERBY and A. DASHMAN, *Clin. Implant Dent. Relat. Res.* **7**(Suppl 1) (2005) S13
38. R. Z. LEGEROS, *Clin. Orthop. Relat. Res.* issue no. (395) (2002) 81
39. M. BOSETTI and E. VERNE, *Biomaterials* **22** (2001) 987
40. A. ROSENGREN and E. PAVLOVIC, *Biomaterials* **23** (2002) 1237
41. M. BOSETTI and V. OTTANI, *Biomaterials* **20** (1999) 363